International Journal of Neural Systems, Vol. 29, No. 5 (2019) 1850032 (15 pages)

DOI: 10.1142/S0129065718500326

World Scientific
www.worldscientific.com

Aberrant Prefrontal–Thalamic–Cerebellar Circuit in Schizophrenia and Depression: Evidence From a Possible Causal Connectivity

Yuchao Jiang*, Mingjun Duan*,†, Xi Chen*, Xingxing Zhang*, Jinnan Gong*, Debo Dong*, Hui Li*,†, Qizhong Yi‡, Shuya Wang§, Jijun Wang¶, Cheng Luo*,‖ and Dezhong Yao*

*The Clinical Hospital of Chengdu Brain Science Institute
MOE Key Lab for Neuroinformation
Center for Information in Medicine
School of life Science and Technology
University of Electronic Science and Technology of China
Chengdu P. R. China

†Department of psychiatry, Chengdu Mental Health Center
Chengdu, P. R. China

‡Psychological Medicine Center
The First Affiliated Hospital of Xinjiang
Medical University, Urumqi, P. R. China

§Biology Department, Emory University, Atlanta, GA, USA

¶Department of EEG Source Imaging
Shanghai Mental Health Center
Shanghai Jiao Tong University School of Medicine
Shanghai, P. R. China

‖chengluo@uestc.edu.cn

Accepted 11 July 2018
Published Online 28 August 2018

Neuroimaging studies have suggested the presence of abnormalities in the prefrontal–thalamic–cerebellar circuit in schizophrenia (SCH) and depression (DEP). However, the common and distinct structural and causal connectivity abnormalities in this circuit between the two disorders are still unclear. In the current study, structural and resting-state functional magnetic resonance imaging (fMRI) data were acquired from 20 patients with SCH, 20 depressive patients and 20 healthy controls (HC). Voxel-based morphometry analysis was first used to assess gray matter volume (GMV). Granger causality analysis, seeded at regions with altered GMVs, was subsequently conducted. To discover the differences between the groups, ANCOVA and post hoc tests were performed. Then, the relationships between the structural changes, causal connectivity and clinical variables were investigated. Finally, a leave-one-out resampling method was implemented to test the consistency. Statistical analyses showed the GMV and causal connectivity changes in the prefrontal–thalamic–cerebellar circuit. Compared with HC, both SCH and DEP exhibited decreased GMV in middle frontal gyrus (MFG), and a lower GMV in MFG and medial prefrontal cortex (MPFC) in SCH than DEP. Compared with HC, both patient groups showed increased causal flow from the right cerebellum to the MPFC (common causal connectivity abnormalities). And distinct causal connectivity abnormalities (increased causal connectivity from the left thalamus to the MPFC in SCH than HC and DEP, and increased causal connectivity from the right cerebellum to the left thalamus in DEP than HC and SCH). In addition, the structural deficits in the MPFC and its causal connectivity from the cerebellum were associated with the negative symptom severity in SCH. This study found common/distinct structural deficits and aberrant causal connectivity patterns in the

‖Corresponding author.

prefrontal–thalamic–cerebellar circuit in SCH and DEP, which may provide a potential direction for understanding the convergent and divergent psychiatric pathological mechanisms between SCH and DEP. Furthermore, concomitant structural and causal connectivity deficits in the MPFC may jointly contribute to the negative symptoms of SCH.

Keywords: Schizophrenia; depression; gray matter; causal connectivity; resting-state fMRI.

1. Introduction

Schizophrenia (SCH) and depression (DEP) are two serious psychiatric disorders that are regarded as distinct entities. However, both disorders share cognitive and affective impairment and even similar clinical features, i.e. the traditional negative symptoms of SCH can conceptually overlap with the common symptoms of DEP.[1] In addition, genetic analyses have identified some common polymorphisms in both disorders.[2] It appears that this evidence began to encourage the investigation of the common pathophysiologies between the two related disorders. By this token, the two diseases may have generally overlapping pathophysiological and disease-specific mechanisms. This study aimed to investigate possible imaging correlates with common/specific transdiagnostic abnormalities.

Recently, the neurobiological alterations in SCH and DEP have been investigated using MRI and (EEG).[3–9] Volumetric reductions in the gray matter of the prefrontal cortex were consistently reported in SCH.[10] Similarly, gray matter loss in prefrontal-related regions, i.e. the right orbitofrontal cortex, dorsolateral prefrontal cortex and the cingulate gyrus, was also observed in DEP.[11] In parallel, studies using functional connectivity have widely investigated the abnormal patterns of the prefrontal–thalamic–cerebellar circuit in SCH.[12–15] A cross-sectional study reported that both refractory and nonrefractory depressive patients showed significantly reduced functional connectivity in prefrontal–limbic–thalamic areas.[16] Based on these evidences, it can be concluded that both disorders show gray matter loss in prefrontal-related regions and in the functional circuits of prefrontal–limbic–thalamic areas. However, it remains unclear whether there are common or distinct causal connectivity abnormalities in this circuit between the two disorders. In addition, a recent study using voxel-based morphometry (VBM) and Granger causality analysis (GCA) demonstrated increased causal connectivity in the prefrontal–thalamic–cerebellar circuit, which may be a compensatory mechanism for combating the structural deficits in SCH[17]; thus, in the current study, we further investigated the relationship between structural deficits, abnormal causal connectivity and symptoms.

As the current investigation is based on the potential transdiagnostic impairments of the prefrontal–thalamic–cerebellar circuit in SCH and DEP, we hypothesized that similar or distinct alterations in this circuit may contribute to a common or diagnostic-specific neurophysiological basis in both disorders. To search for a potential transdiagnostic neural signature, multimodal MRI was performed to assess both structural and functional features.[18–22] We first used VBM analysis[23] to evaluate the whole-brain GMVs among two groups of patients and healthy controls (HC). Next, the regions with altered GMVs were selected for further causal connectivity analysis using GCA.[24] Unlike certain other functional connectivity methods which characterize undirected connectivity by estimating temporal synchronization,[25,26] GCA is a method based on linear regression for investigating whether the past value of the time series in one region could predict the current value of time series in another region and thus can reveal the direction of information flow.[24] Then, we also examined whether these structural and functional abnormalities were correlated with clinical variables. Finally, we implemented a leave-one-out resampling method to test the consistency of the present study using a subset $(n-1)$ of subjects.

2. Methods

2.1. *Participants*

Twenty patients with SCH, 20 depressive disorder patients and 20 HC were recruited from Chengdu Mental Health Center. The inclusion criterion for

patients included: (1) Each patient was diagnosed according to the Diagnostic and Statistical Manual of Mental Disorders, Fourth Edition (DSM-IV) by two experienced clinical psychiatrists; (2) All subjects from age 18 to 55 years; (3) No contraindications to MRI scanning. The exclusion criterion for patients included: (1) A history of brain structural abnormality, substance-related disorders, major medical or neurological disorder; (2) patients with pregnancy or lactation were excluded; (3) Considering the genetic effect, if more than one patient from the same family, only one patient was included in this study; (4) SCH patients with a history of depressive episode were excluded. The inclusion criterion for HC included: (1) Age from 18 to 55 years; (2) No contraindications to MRI scanning; (3) All HC subjects took no hormones or psychoactive substances in at least six months. The exclusion criterion for HC included: (1) A history of brain structural abnormality, substance-related disorders, major medical or neurological disorder; (2) subjects with pregnancy or lactation were excluded; (3) The history of psychiatric disorder in a first- or second-degree relative was an additional exclusion criterion for HC to exclude the potential effect of genetic backgrounds. All patients were on medication, e.g. antipsychotics for SCH and antidepressants for DEP. 20 patients with SCH received atypical and typical antipsychotics (olanzapine ($n = 1$), clozapine ($n = 3$), quetiapine ($n = 4$), risperidone ($n = 3$), ziprasidone ($n = 1$), aripiprazole ($n = 1$), sulpiride ($n = 1$), clozapine and risperidone ($n = 2$), risperidone and ziprasidone ($n = 1$), clozapine and aripiprazole ($n = 2$), risperidone and aripiprazole ($n = 1$), risperidone and sulpiride ($n = 1$), quetiapine and sulpiride ($n = 1$), clozapine and sulpiride ($n = 1$)). The chlorpromazine equivalent dose of the antipsychotics was 281.2 (mean value) $\pm$122.7 (standard deviation) mg/day. In addition, five SCH patients received benzodiazepines (clonazepam (2 mg/day), alprazolam (4–8 mg/day)), two received anti-epileptic medication as mood-stabilizers (sodium valproate (0.6 g/day)). Of the 20 patients with DEP, 1 received tricyclic antidepressants (TCA) (amitriptyline (100 mg/day)), 15 received serotonin reuptake inhibitors (SSRI)(paroxetine (10–50 mg/day), trazodone (25–125 mg/day), escitalopram (5–20 mg/day), fluoxetine (20 mg/day)), four received serotonin norepinephrine reuptake inhibitors (SNRI) (venlafaxine (75–150 mg/day)). In addition, three patients received anti-epileptic medication as mood-stabilizers (lamotrigine (12.5–50 mg/day), sodium valproate (500 mg/day)), five atypical antipsychotics (aripiprazole (20 mg/day), amisulpride (1 g/day), quetiapine (50–200 mg/day)), 15 benzodiazepines (estazolam (1 mg/day), lorazepam (0.5–2 g/day), clonazepam (2 mg/day)) and 7 non-benzodiazepines (tandospirone (30 mg/day), buspirone (15–30 mg/day)). Symptoms severity was assessed using the Positive and Negative Syndrome Scale (PANSS) for each patient with SCH and the 24-item Hamilton Rating Scale (HAMD-24) in the DEP group. Age, gender, education information and symptoms scores are provided in Table 1. The study was approved by the Ethics Committee of Chengdu Mental Health Center. Written informed

Table 1. Demographic and Clinical Characteristics.

	Schizophrenia Mean(SD)	Depression Mean(SD)	Healthy Controls Mean(SD)	*P*-value
Gender(male/female)	9/11	7/13	7/13	0.754[a]
Age(years)	40.3(13.8)	41.8(14.2)	41.6(13.6)	0.931[b]
Education(years)	11.0(2.7)	11.3(2.6)	10.3(3.0)	0.305[b]
PANSS				
Positive score	12.9(5.6)	—	—	—
Negative score	18.0(7.0)	—	—	—
General score	27.8(5.3)	—	—	—
Total score	58.7(12.5)	—	—	—
HAMD-24	—	5.3(1.3)	—	—

Note: [a]Chi-square test and [b]Kruskal–Wallis tests were used to assess group differences for various variable types.

consent was obtained after complete description of the study from all HCs and their legal guardian for patients.

2.2. *Data acquisition*

A 3-Tesla MRI scanner (GE DISCOVERY MR 750, USA) with an eight channel-phased array head coil was used to collect imaging data in the University of Electronic Science and Technology of China. The structural images (T1-weighted) and resting-state functional MRI (fMRI) of the whole-brain were acquired for all subjects. The three dimensional fast spoiled gradient echo (T1-3D FSPGR) sequence was used for high-spatial-resolution T1-weighted axial anatomical images. The main parameters include: repetition time (TR) = 6.008 ms; echo time (TE) = 1.984 ms; flip angle (FA) = 90°; field of view (FOV) = 25.6 cm × 25.6 cm; matrix size = 256 × 256; slice thickness = 1 mm (no gap). Gradient-echo echo-planar imaging (EPI) sequence was used to acquire resting-state functional images. The scan parameters were as following: TR = 2 s; TE = 30 ms; FA = 90°; FOV = 24 cm × 24 cm; matrix size = 64 × 64; slice thickness = 4 mm (no gap). Resting-state functional scanning lasted 510 s. When capturing images, in order to minimize head motion, foam pads were used to fix their heads; and ear plugs were used to reduce uncomfortableness of scanning noise. All participants were instructed to keep minds wandering and eyes closed without falling asleep during fMRI scanning. All subjects were also surveyed whether they fell asleep during scanning.

2.3. *Structural data analysis*

Imaging data were analyzed with standard steps of VBM analysis[27] in Statistical Parametric Mapping (SPM, http://www.fil.ion.ucl.ac.uk/spm/). First of all, we check all images for artifacts, and reoriented so that the image origins were set at the anterior commissure. Subsequently, T1-weighted images were segmented into gray matter, white matter (WM) and cerebrospinal fluid (CSF), and total volume of gray matter which was used to estimate the true volume of the tissue was obtained in the native space for each subject. Then, DARTEL approach was used for optimal registration of individual segments to a group mean template. The segments were modulated by the Jacobian determents to correct for volume changes in nonlinear normalization. The modulated segments were further normalized to the Montreal Neurological Institute space and smoothed using an 8 mm full-width at half maximum (FWHM) Gaussian kernel.[28] The generated smoothed, modulated nonlinear only, warped, segmented gray matter images allowed comparing the absolute amount of tissue and were used as the GMV for subsequent group comparisons.

After normality tests, total volumes of gray matter, WM volume and whole brain were compared among the three groups using ANOVA, respectively. Voxel-wise comparisons of GMV were analyzed using ANCOVA with age, gender, education and total volume of whole brain as covariates of no interest. A gray matter majority optimal threshold mask, created from all subjects, was applied to eliminate voxels of nongray matter.[29] For multiple comparisons correction, we maintained a corrected false-positive detection rate of $P_{\text{corrected}} < 0.05$ using a voxel threshold of $P < 0.001$ and a cluster extent threshold determined by Gaussian Random Field theory. For these regions with significant group differences from ANCOVA, the mean GMV of each region was extracted to perform *post-hoc* least significant difference (LSD) analysis.

2.4. *Functional data preprocessing*

The functional data preprocessing was performed using the DPABI toolbox (http://rfmri.org/dpabi).[30] Imaging data preprocessing steps consisted of 1) removing the first five volumes to allow the subjects' adaptation to the scanning environment and make signal equilibrium, 2) slice timing, 3) realignment, 4) coregistering T1 image to functional space and segmenting using DARTEL,[31] 5) regressing out nuisance signals (including 24-parameter motion model, first five principal components signals of WM and CSF, and linear trend), 6) data scrubbing[32] by modeling the "bad" time point (framewise displacement [FD] > 0.5) as a separate regressor in nuisance covariates regression. 7) normalizing the functional images into the MNI space using unified segment T1 image information[33] and then resampling to 3 × 3 × 3 mm^3, 8) band-pass filtering (0.01–0.1 Hz), 9) smoothing (FWHM = 6 mm). We did not regress out global mean signal because it can distort between-group comparisons of

inter-regional correlation.[34] Motion-related artifacts were not only controlled using higher-order regression model and data scrubbing approaches at the individual-level, but also assessed for the differences of head motion at the group-level by traditional statistical analyses. All participants' head motions of translation and rotation were less than 2 mm and 2°. The z-translation motion parameters showed significant group effect (max: $F = 4.81$, $P = 0.012$ and mean: $F = 3.79$, $P = 0.028$). Therefore, the z-translation motion parameters were used as covariates of no interest in the following group-level statistical analyses.

2.5. *Causal causality analysis*

In this study, auto regressive models were utilized to estimate the Granger causality to investigate whether the past value of one time series could correctly predict another.[35] While combining the information of the past values of the time series, X and Y can better estimate the current value of Y than the past value of Y alone, the time series X has a causal effect on time series Y. Consistent with previous GCA definitions,[24] the GCA features are briefly described here. For the auto regressive representation:

$$Y_t = \sum_{i=1}^{p} m_i Y_{(t-i)} + \varepsilon_t, \tag{1}$$

$$\mathrm{var}(\varepsilon_t) = U_1, \tag{2}$$

$$X_t = \sum_{i=1}^{p} m'_i X_{(t-i)} + \varepsilon'_t, \tag{3}$$

$$\mathrm{var}(\varepsilon'_t) = V_1, \tag{4}$$

where ε_t and ε'_t are the residuals of formulas (1) and (3); U_1 and V_1 are the variances of ε_t and ε'_t, respectively.

$$Y_t = \sum_{i=1}^{p} a_i X_{(t-i)} + \sum_{i=1}^{p} b_i Y_{(t-i)} + \mu_t, \tag{5}$$

$$\mathrm{var}(\mu_t) = U_2, \tag{6}$$

$$X_t = \sum_{i=1}^{p} a'_i Y_{(t-i)} + \sum_{i=1}^{p} b'_i X_{(t-i)} + \mu'_t, \tag{7}$$

$$\mathrm{var}(\mu'_t) = V_2, \tag{8}$$

where μt and $\mu t'$ are the residuals of formula (5) and (7); U_2 and V_2 are the variances of μ_t and μ'_t, respectively.

$$F_{x\to y} = \ln \frac{U_1}{U_2}, \tag{9}$$

$$F_{y\to x} = \ln \frac{V_1}{V_2}, \tag{10}$$

$$F_{\mathrm{net}} = F_{x\to y} - F_{y\to x}. \tag{11}$$

The specific parameters of $F_{X\to Y}$ (formula 9) and $F_{Y\to X}$ (formula 10) are introduced to further describe the causal effect based on the decrease in the variance of the residuals.[24] Each parameter is given by the logarithm of a particular variance ratio between the residuals of the regressive model of X added to the past description of Y and of the residuals variance of Y alone. $F_{X\to Y}$ (or $F_{Y\to X}$) represents the amount of causality given by X (or Y) when applied to the prediction of Y (or X). Additionally, the F_{net} (formula 11) which was defined as the subtraction of $F_{X\to Y}$ from $F_{Y\to X}$ was used to measure the flow difference term of the net influence.[36] Positive F_{net} values indicated that the influence was from X to Y, whereas negative values pointed to an influence in the reverse direction.

Based on the abovementioned VBM analysis, the regions that showed significant group differences were defined as the seeds. The peak voxel of each seed was chosen as a 6-mm-radius sphere seed for the GCA. The voxelwise, residual-based GCA was performed on the gray matter mask using REST toolbox (http://www.restfmri.net).[37] This GCA method has been used in our previous study which identified an altered hippocampo–cerebello–cortical circuit in SCH.[38] This previous study indicated that the GCA could be an effective measure to investigate the abnormal effective connectivity in psychiatry disorders. Different from the previous study, the current study applied the GCA to investigate the altered connectivity based on the structural deficits in a different sample of SCH, DEP and HC. Same as our previous study,[38] three cause parameters ($F_{X\to Y}$, $F_{Y\to X}$ and F_{net}) including inflow-to-seed, outflow-from-seed and out-inflow were calculated in the current study. For each seed, three maps were acquired between the seed and each voxel in the gray matter mask. The resulting $F_{X\to Y}$, $F_{Y\to X}$ and F_{net} were further transformed to an approximately

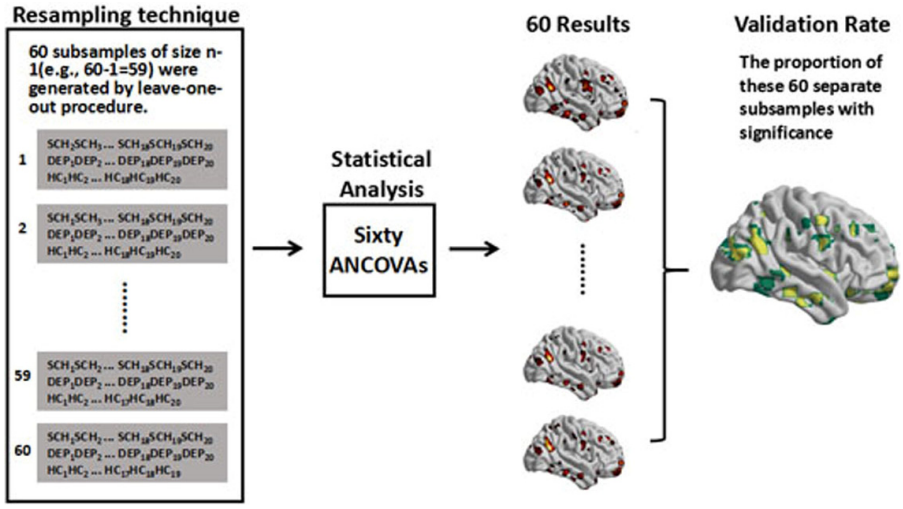

Fig. 1. A schematic of leave-one-out resampling procedure in statistical test.

normal distribution and were then converted to z-scores, which could better improve the normality for the subsequent statistical analyses.[35]

To discover the differences between the groups, ANCOVA and *post hoc* LSD tests were performed with the sex, age, education and head motion variables as unconcerned covariates. Multiple comparison correction was also performed using the same parameter described above ($P_{\text{corrected}} < 0.01$ due to four seeds).

2.6. *Correlations between altered GMV, causal effect and clinical variable*

The altered GMV and causal effect of interested were defined based on the results of above VBM and GCA and then extracted for the correlation analysis. The averaged GMV of each ROI were correlated with clinical features (HAMD and PANSS positive, negative, general psychopathology subscales and total scores) using partial correlation analysis when controlling the effects of age, gender, education and total volume of gray matter. In addition, the causal effect showing significant difference between groups were correlated with clinical features by partial correlation when controlling the effects of age, gender, education and head-motion variables. We also examined the correlations between the altered GMV and causal effects using partial correlation when controlling the effects of age, gender, education, total volume of gray matter and head motion variables.

2.7. *Leave-one-out resampling validation*

A leave-one-out resampling method was used to assess whether the above results were driven by a single subject from any of the 3 groups. For each voxel, sixty separate subsamples of size $n-1$ (e.g. $60-1=59$) were generated by leave-one-out resampling procedure and each subsample was performed using ANCOVA to assess significance ($p < 0.001$). For each voxel, the validation rate (VR) was the proportion of these 60 separate subsamples with significance. A high VR represents that the results are not dependent on some specific outliers. The Fig. 1 provided a schematic of leave-one-out resampling procedure.

3. Results

3.1. *Demographic and clinical variables*

Three groups had no difference in gender (Chi-square test, $p = 0.754$), age (Kruskal–Wallis test, $p = 0.931$) and education (Kruskal–Wallis test, $p = 0.305$). There was a significant difference in disease duration (Mann–Whitney test, $p = 0.016$) between two patient groups. Detailed information can be seen in Table 1.

3.2. *Voxel-based morphometric analysis*

The total volumes of the gray matter, WM and whole brain exhibited no significant differences among the

groups ($p > 0.3$). ANCOVA showed four clusters with significant group effects in the GMV ($P_{\text{corrected}} < 0.05$).

The *post hoc* analysis-based ANCOVA revealed that compared with the HCs, both of the patient groups showed significantly decreased GMV in the bilateral middle frontal gyrus (MFG). Moreover, SCH showed significantly lower GMV in the bilateral MFG than DEP. Additionally, SCH had significantly decreased GMV in the medial prefrontal cortex (MPFC) and rectus than both DEP and HCs. The results are presented in Fig. 2 and Table 2.

3.3. *Granger causality analyses*

Based on the differences found through the GMV analysis, four ROIs, including the bilateral MFG, MPFC and rectus were selected as seeds for the GCA.

For the comparisons of the inflow-to-seed maps, ANCOVA showed an alteration in the causality effect for seeds in the MPFC ($P_{\text{corrected}} < 0.01$, based on four seeds) (Fig. 3 and Table 3). *Post hoc* analysis revealed that SCH showed increased causal flow from the left thalamus to the MPFC, while no difference was observed in DEP.

For the comparisons of the out-inflow-to-seed maps, ANCOVA showed an alteration in the causality effect of the seeds in the MPFC ($P_{\text{corrected}} < 0.01$, based on four seeds) (Fig. 3 and Table 3). *Post hoc* analysis revealed that compared with the HCs, both SCH and DEP showed significantly increased outinflow from the right cerebellum to the MPFC.

For the comparisons of the outflow-to-seed maps, ANCOVA showed an alteration in the causality effect of the seeds in the right MFG ($P_{\text{corrected}} < 0.01$, based on four seeds) (Fig. 3 and Table 3). *Post hoc* analysis revealed that only SCH showed significantly increased flow from the right MFG to the left IFG. Above results exhibited altered connectivity from the thalamus to the prefrontal cortex in SCH and common altered connectivity from the cerebellum to the prefrontal cortex in SCH and DEP. As the thalamus is anatomically the relaying node in the link between the cerebellum and cortex, we also evaluated the causal effect between the left thalamus and right cerebellum using a region-to-region GCA of the three groups. The peak voxels of the left thalamus $(-91, -24, 0)$ and right cerebellum $(27, -45, -18)$ were chosen as 3 mm-radius sphere ROIs for the GCA. The $F_{X\to Y}$, $F_{Y\to X}$ and F_{net} were calculated to estimate the causal effect between the two ROIs.

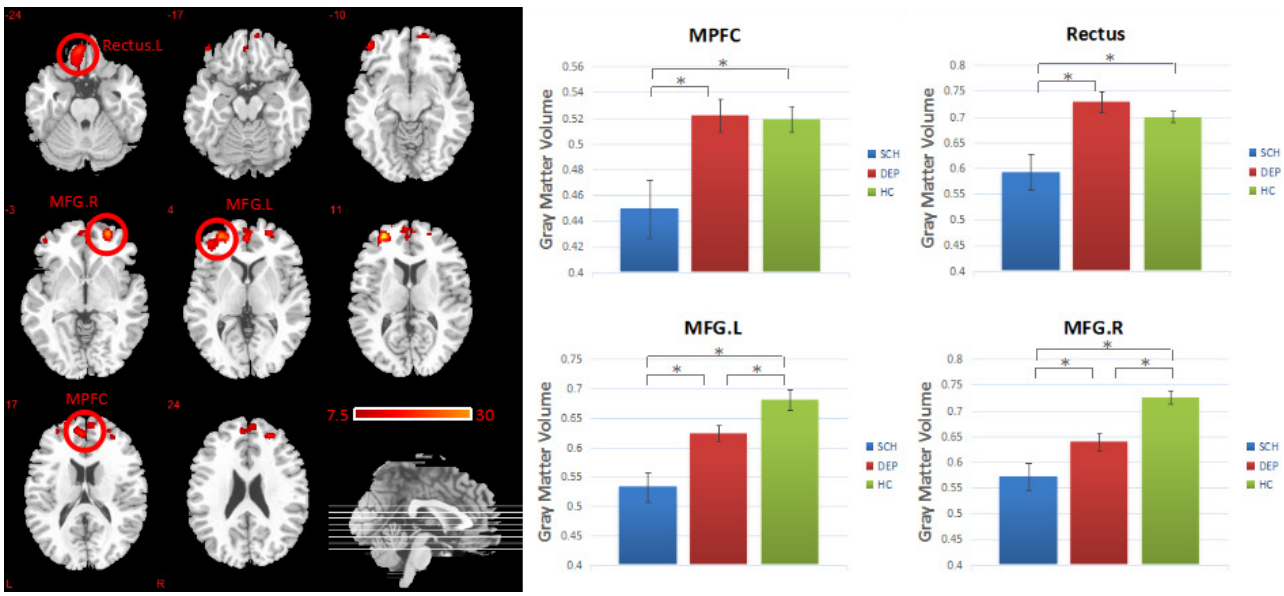

Fig. 2. Differences of gray matter volume in SCH, DEP and HC by the ANCOVA. Color bars represent F values. Post-hoc analyses showed reduced gray matter volume of MPFC, rectus and bilateral MFG in patients with SCH.
Abbreviations: SCH: schizophrenia, DEP: depression, HC: healthy controls, MFG: middle frontal gyrus, MPFC: medial prefrontal cortex.

Table 2. Regions with significantly decreased gray matter volume in patients with schizophrenia and depression.

Regions	MNI Coordinates	Mean(SE) Gray Matter Volume			Main Effect of ANCOVA			*Post-hoc* LSD *P* Value
		SCH	DEP	HC	F(P) Value	Cluster (mm^3)	Validation rate	
MPFC	$-1, 51, 18$	0.45 (0.023)	0.52 (0.013)	0.52 (0.010)	13.6 (1.7×10^{-5})	3058	81.55%	$P(\text{SCH} < \text{DEP}) = 6.4 \times 10^{-5*}$ $P(\text{SCH} < \text{HC}) = 1.1 \times 10^{-4*}$ $P(\text{DEP} > \text{HC}) = 0.87$
Rectus.L	$-4, 43, -24$	0.59 (0.035)	0.73 (0.020)	0.70 (0.011)	14.3 (1.1×10^{-5})	2808	89.67%	$P(\text{SCH} < \text{DEP}) = 1.3 \times 10^{-5*}$ $P(\text{SCH} < \text{HC}) = 3.8 \times 10^{-4*}$ $P(\text{DEP} > \text{HC}) = 0.31$
MFG.L	$-27, 54, 9$	0.53 (0.025)	0.62 (0.015)	0.68 (0.017)	27.3 (7.2×10^{-9})	3632	90.94%	$P(\text{SCH} < \text{DEP}) = 3.4 \times 10^{-5*}$ $P(\text{SCH} < \text{HC}) = 1.1 \times 10^{-9*}$ $P(\text{DEP} < \text{HC}) = 6.0 \times 10^{-3*}$
MFG.R	27,57,0	0.57 (0.026)	0.64 (0.017)	0.73 (0.014)	22.6 (8.0×10^{-8})	1974	91.42%	$P(\text{SCH} < \text{DEP}) = 4.0 \times 10^{-3*}$ $P(\text{SCH} < \text{HC}) = 7.5 \times 10^{-9*}$ $P(\text{DEP} < \text{HC}) = 3.2 \times 10^{-4*}$

Abbreviations: SCH: schizophrenia, DEP: depression, HC: health controls, L: left, R: right, MPFC: medial prefrontal cortex, MFG: middle frontal gyrus.

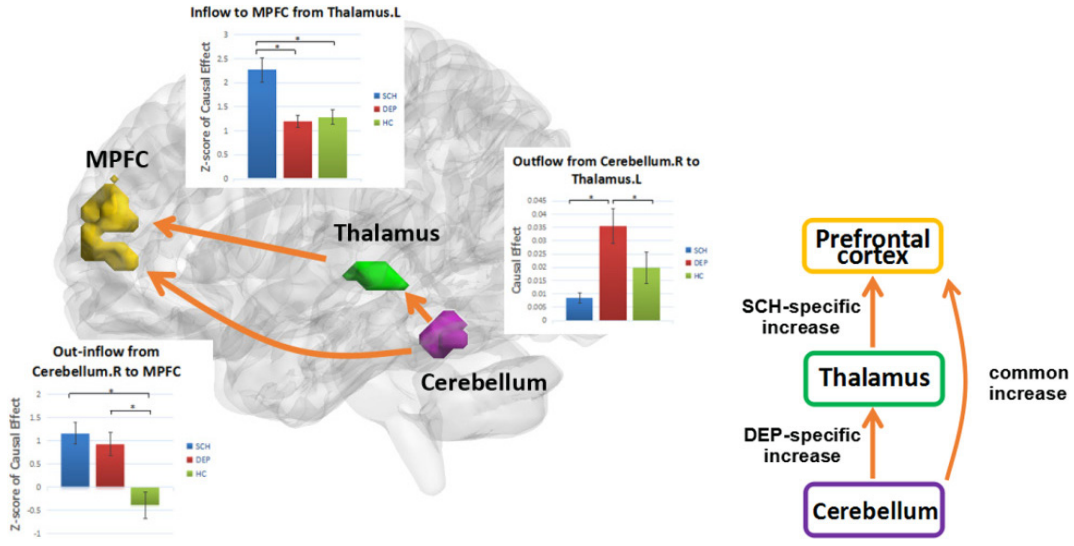

(a) (b)

Fig. 3. Causal connectivity assessed by Granger causality analysis. (a) Causal connectivity changes in patients with SCH, DEP and HC. (b) A model showing the common/distinct causal connectivity of the prefrontal–thalamic–cerebellar circuit in SCH and DEP.
Abbreviations: SCH: schizophrenia, DEP: depression, HC: healthy controls, MPFC: medial prefrontal cortex.

As the $F_{X \to Y}$, $F_{Y \to X}$ and F_{net} from the ROI-to-ROI GCA cannot be transformed to z-scores, the Kruskal–Wallis H test was used to determine the group differences, and the Mann–Whitney U test was performed to compare the differences between any two of the groups. The nonparametric tests were performed using SPSS. The results showed significant group differences in the causal connectivity from the right cerebellum to the left thalamus (Kruskal–Wallis test, $p = 0.005$). *Post hoc* analysis demonstrated that DEP had significantly higher causal connectivity from the right cerebellum to the left

Table 3. Regions with significant group differences between schizophrenia, depression and the healthy controls in the effective connectivity analysis.

Regions	MNI Coordinates	Mean(SE) Z Score of Causal Effect			Main Effect of ANCOVA			*Post-hoc* LSD *P* Value
		SCH	DEP	HC	F(P) Value	Cluster (mm^3)	Validation rate	
Causal inflow to the seed of MPFC								
Thalamus.L	$(-9, -24, 0)$	2.3 (0.253)	1.2 (0.134)	1.3 (0.15)	10.70 (1.3×10^{-4})	432	88.02%	$p(\text{SCH} > \text{DEP}) = 1.6 \times 10^{-4*}$ $p(\text{SCH} > \text{HC}) = 4.9 \times 10^{-4*}$ $p(\text{DEP} < \text{HC}) = 0.74$
Causal out-inflow to the seed of MPFC								
Cerebellum.R	$(27, -45, -18)$	1.2 (0.233)	0.93 (0.246)	−0.38 (0.285)	11.97 (5.3×10^{-5})	1323	88.16%	$p(\text{SCH} < \text{DEP}) = 0.51$ $p(\text{SCH} < \text{HC}) = 6.4 \times 10^{-5*}$ $p(\text{DEP} < \text{HC}) = 5.3 \times 10^{-4*}$
Causal outflow from the seed of right MFG								
IFG	$(-21, 19, -12)$	2.4 (0.316)	1.2 (0.187)	1.1 (0.127)	12.05 (5.0×10^{-5})	702	81.35%	$p(\text{SCH} > \text{DEP}) = 2.5 \times 10^{-4*}$ $p(\text{SCH} > \text{HC}) = 1.1 \times 10^{-4*}$ $p(\text{DEP} > \text{HC}) = 0.80$

Abbreviations: SCH: schizophrenia, DEP: depression, HC: healthy controls, L: left, R: right, MPFC: medial prefrontal cortex, MFG: middle frontal gyrus, IFG: inferior frontal gyrus.

thalamus than SCH (Mann–Whitney test, $p = 0.001$) and the HCs (Mann–Whitney test, $p = 0.021$), while SCH and the HCs showed no significant differences (Mann–Whitney test, $p = 0.607$).

In short, this study observed common increased causal connectivity from cerebellum to MPFC in both patient groups and DEP-specific increased causal connectivity from cerebellum to thalamus as well as SCH-specific increased causal connectivity from thalamus to MPFC (Fig. 3(B)).

3.4. *Correlations between Altered GMV, causal effect and clinical variable*

We investigated the correlation between the altered GMV, causal effect and clinical variables for each

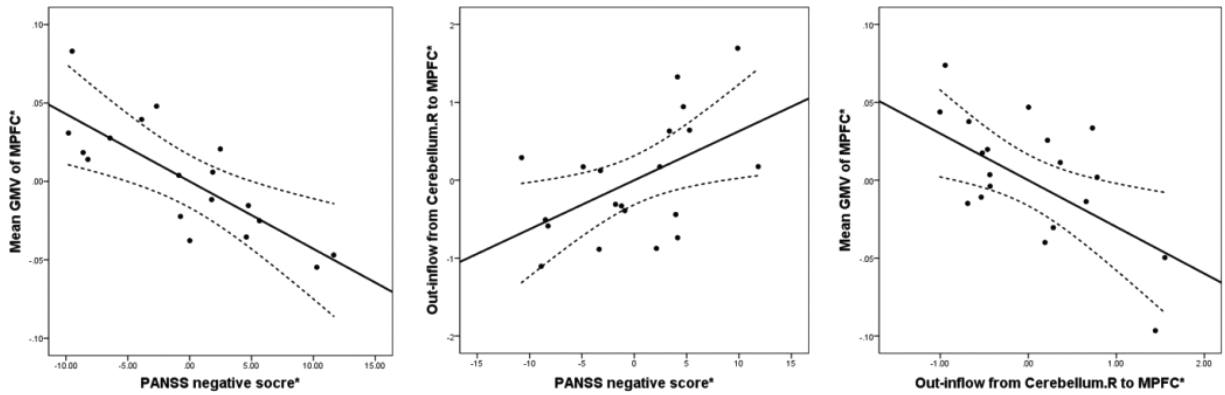

Fig. 4. Correlations between the structural deficits, causal effects and symptom severity in schizophrenia. * represent the adjusted values when controlling for the influence of age, gender, education level, total brain volume and head-motion variables. The punctured curves represent a 95% confidence interval.
Abbreviations: GMV: gray matter volume, MPFC: medial prefrontal cortex, PANSS: Positive and Negative Symptom Scale.

patient group. Results showed that in the SCH group, the GMV of MPFC had a significant negative correlation with the PANSS negative subscales scores ($R = -0.615, p = 0.011$, Fig. 4) and the causal out-inflow from the right cerebellum to the MPFC had a significant positive correlation with the PANSS negative subscales scores ($R = 0.518$, $p = 0.047$, Fig. 4). In addition, we also found the significant negative correlation between the GMV in the MPFC and the causal out-inflow from the right cerebellum to the MPFC ($R = -0.550$, $p = 0.042$, Fig. 4). No significant correlation between altered GMV, causal effect and clinical variables was observed in the DEP group.

3.5. *Leave-one-out resampling validation*

Almost all voxels of clusters with significant group differences based on GMV analysis and GCA analysis exhibited a perfect consistency (VR = 100%) of the present study by a subset $(n-1)$ of patients. The mean VR of each cluster showed an excellent validation rate (all VRs $> 80\%$). It showed that the results had a high consistency.

4. Discussion

Although many studies have demonstrated abnormalities in the prefrontal–thalamic–cerebellar circuit in SCH and DEP, to the best of our knowledge, this study is the first to directly investigate the common and distinct abnormalities of this circuit between two disorders using a combination of neuroanatomical features and causal connectivity analysis. The following are the three major results of this study: first, a lower GMV of the prefrontal cortex was observed in both SCH and DEP. Although both patient groups exhibited significantly decreased GMV in the bilateral MFG, SCH had a significantly lower GMV than DEP. In addition, only SCH had a significantly decreased GMV in the MPFC and rectus. Moreover, the GMV of the MPFC was negatively correlated with the negative symptom severity in SCH. Second, both SCH and DEP had a higher causal out-inflow from the cerebellum to the MPFC than the HCs. Interestingly, this enhanced causal out-inflow showed a negative correlation with the decreased GMV in the MPFC and was positively related with the symptom severity (PANSS negative score) in SCH. Finally, distinct causal connectivity abnormalities were found in SCH and DEP; namely, increased causal connectivity from the thalamus to the MPFC was observed only in SCH, and increased causal connectivity from the cerebellum to the thalamus was noted only in DEP.

4.1. *Structural deficits in the prefrontal cortex*

Consistent with the findings of previous studies of DEP[39] and SCH,[10] the reductions in the GMV of the prefrontal cortex were further demonstrated in the current study. A body of studies have reported that reduced prefrontal GMV is linked to executive dysfunction in SCH. Although both types of patients showed decreased GMV in the bilateral MFG, a lower GMV was found in SCH than in DEP here, which might imply varying degrees of structural impairment and the progression of pathophysiology in different psychological disorders. In addition, we observed a schizophrenia-specific reduction in the GMV of the MPFC, which provided further evidence of the structural deficits in the MPFC in SCH.[17,40] Recently, a meta-analysis confirmed opposing resting-state activities (hypoactivation in SCH and hyperactivation in DEP) in the MPFC,[41] which may be in line with a different dysfunction in self-reference.[42–44] Furthermore, the reduced GMV in the MPFC had a negative correlation with the PANSS negative score. Based on previous reports, negative symptoms have a greater impact on functioning[45] and resistance to treatment with antipsychotropic drugs.[46] Thus, the different structural deficits in the MPFC may be a potential foundation of different functional activity. Moreover, some studies have attempted to discriminate between patients and HCs and between patients with different psychotic behaviors using machine learning based on anatomical structures[47] and fMRI.[48–51] Our findings may provide help in the classification of patients with SCH and DEP.

4.2. *Common causal connectivity abnormalities from the cerebellum to the prefrontal cortex*

Although SCH and DEP are regarded as two distinct psychiatric disorders from a traditional viewpoint, some studies have also provided a possible

direction for investigating potential similar symptoms and presumptive common pathologies between SCH and DEP. For example, Muller *et al.*[52] suggested that the neurobiology of depressive symptoms in SCH might be similar to that in DEP. The dysfunction in the frontal cortex may contribute to the depressive symptoms in SCH.[53] Interestingly, in the current study, increased out-inflow connectivity was observed from the cerebellum to the prefrontal cortex in both SCH and DEP. The change, which was the same in both patient groups and was located in similar anatomic regions, was defined as a common alteration. The results are similar to those of a previous study, which found increased prefrontal–cerebellar causal connectivity.[17] At first glance, it seemed that the increased effective connectivity appeared inconsistent with the general notion that functional connectivity is reduced overall in SCH.[54] However, the results provided positive evidence for the neurodevelopmental model. Previous studies have proposed that the connection of the circuit across the lifespan can be expressed as an inverted U-curve, with maximal connectivity occurring in adolescence.[17,55] The inverted U-curve suggests an abrupt transition of this circuit from adolescence to adulthood. From this viewpoint, the increased causal connectivity exhibited in SCH and DEP may result from the abnormal development and refinement of the prefrontal–thalamic–cerebellar circuit, which might contribute to atypical brain maturation in patients. In addition, this result was consistent with the previous finding that the cerebellum is recruited to participate in abnormal information flow of the frontal–thalamic–cerebellar circuit in SCH.[17] Combined with the above findings that SCH and DEP showed abnormal information flow in the prefrontal–thalamic–cerebellar circuit (increased flow from the thalamus to the MPFC in SCH and increased flow from the cerebellum to the thalamus in DEP), the cerebellum may provide response feedback to the prefrontal cortex when abnormalities in the information flow occur in the prefrontal–thalamic–cerebellar circuit. Taken together, abnormal causal connectivity from the cerebellum to the prefrontal cortex might be a possible evidence for the understanding of transdiagnostic pathological mechanisms from the perspective of the neuroimaging.

In addition, the increased out-inflow from the cerebellum to the MPFC was also negatively correlated with the GMV of the MPFC in SCH. We presumed that the increased causal flow from the cerebellum to the MPFC might be a compensatory effort to combat the structural deficits in the MPFC. Meanwhile, increased out-in flow from the cerebellum to the MPFC was positively related to the PANSS negative score of the patients with SCH. Combined with the correlation between the GMV of the MPFC and PANSS negative score, the causal connectivity of the prefrontal–thalamic–cerebellar circuit might be partly affected by structural deficits, which contribute to the negative symptoms in SCH.

4.3. *Distinct causal connectivity between SCH and DEP*

Some neuroimaging studies have found disease-specific dysconnectivity patterns between SCH and DEP. For example, Schilbach *et al.*[56] found reduced connectivity between the MPFC and the parietal operculum in SCH relative to DEP. Yu *et al.*[57] found that the connections between the prefrontal cortex and the affective network differed in SCH and DEP. A notable finding of the present study was the different abnormalities in the causal connectivity with the MPFC between SCH and DEP. In detail, increased causal connectivity from the thalamus to the MPFC and from the right MFG to the left IFG were only observed in SCH, and increased causal connectivity from the cerebellum to the thalamus was only noted in DEP.

Consistent with previous research, our results verified the occurrence of significant changes in the prefrontal–thalamic connectivity in SCH. Although many studies have suggested the presence of lower prefrontal–thalamic functional connectivity in SCH,[12,58] increased causal connectivity between these regions has also been reported in some studies. For example, Wagner *et al.*[59] found increased endogenous connectivity between the prefrontal cortex and thalamus using dynamic causal modeling, potentially suggesting compensatory hyperconnectivity according to the reduced BOLD signal in the corresponding regions. In addition, broad evidence from diffusion tensor imaging has indicated the presence of decreased prefrontal–thalamic structural connectivity in SCH.[60] Therefore, the higher causal connectivity from the thalamus to the prefrontal cortex

may be a compensatory effort to combat the structural deficits.

To our knowledge, no study has reported abnormal causal connectivity from the cerebellum to the thalamus in DEP. However, structural deficits of the thalamus and cerebellum have been observed in DEP.[61] A novel computational meta-analysis summarized gray matter reductions in the thalamus and cerebellum,[61] which may contribute to dysfunction in the generation and regulation of emotions in DEP. The thalamus, as a complex information integration node, has been demonstrated to be involved in multisensory emotion recognition and processing.[62] Although the cerebellum was initially considered to be associated with motor coordination, it is now known to participate in extensive emotional processing[62] and is referred to as the "emotional pacemaker".[63] Hence, the altered causal connectivity from the cerebellum to the thalamus might be related to the emotional impairment in DEP.

4.4. *Limitations*

This study had several limitations. First although an almost perfect consistency was demonstrated by a leave-one-out resampling validation analysis, a larger number of participant samples is needed to increase the reliability and sensitivity in the future. Second, both the SCH and DEP patients were taking psychotropic medication, and two of the groups showed significant differences in disease duration, which may introduce confounding effects to some extent. In addition, the neuropsychological assessment was not evaluated, so we can only infer that the changed GMV and causal connectivity are associated with the general pathophysiology. Additionally, recent studies have suggested that the thalamus is not a single brain area with a unitary structure and function; thus, it is crucial to further examine abnormalities of the structure and function of specific thalamic nuclei in the future. Finally, although GCA has been widely used in fMRI studies, it is still controversial because the temporal resolution is too low for realistic neural communication,[64] which is also a common limitation for both GCA and other connectivity analysis such as functional connectivity in the fMRI studies. This study observed altered effective connectivity between the cerebellum and cortex; however, no neural circuits were responsible for the connection. Thus, the results from the GCA should be carefully interpreted. In addition, other measures that assess brain dynamics[50,65,66] should be considered in the future. The results obtained in the first step of the VBM analysis had an influence on the connectivity analysis performed in the second step. Finally, previous study reported that DEP patients with psychotic symptoms had more overlap with SCH in terms of structural and functional changes than nonpsychotic DEP patients;[67] thus, the distinction between psychotic and nonpsychotic DEP patients should be considered in future work.

4.5. *Conclusion*

Combining VBM analysis and causal connectivity analysis, the current study found common/distinct structural deficits and aberrant causal connectivity patterns in the prefrontal–thalamic–cerebellar circuit in SCH and DEP, which may provide a potential direction for the understanding of the transdiagnostic pathological mechanisms. Common dysconnectivity might suggest the aberrant development and refinement of this circuit, which might contribute to atypical brain maturation in two disorders. Disorder-specific alterations also exist as a graded manner of impairment by more serious structural deficit in the prefrontal cortex in SCH as compared to DEP. In particular, correlations between the prefrontal structural deficits, causal connectivity and negative symptoms were observed in SCH, suggesting a partial effect of the structural deficits on this circuit, which may jointly contribute to the negative symptoms of SCH. These findings provided evidence for the convergent and divergent transdiagnostic abnormalities in the prefrontal–thalamic–cerebellar circuit, which may contribute to the common/specific neurophysiological basis in two disorders.

Note Added in Proof

This study is our original unpublished work and the manuscript or any variation of it has not been submitted to another publication previously.

Acknowledgments

This study was funded by grants from National Nature Science Foundation of China (81330032, 81471638, 81771822, 81571759) and the Project of Science and Technology Department of Sichuan Province (2017HH0001 and 2017SZ0004).

References

1. M. Sostaric and B. Zalar, The overlap of cognitive impairment in depression and schizophrenia: A comparative study, *Psychiatr. Danub.* **23** (2011) 251–256.
2. Cross-Disorder Group of the Psychiatric Genomics Consortium, Identification of risk loci with shared effects on five major psychiatric disorders: A genome-wide analysis, *Lancet* **381** (2013) 1371–1379.
3. M. Ahmadlou, H. Adeli and A. Adeli, Spatiotemporal analysis of relative convergence of EEGs reveals differences between brain dynamics of depressive women and men, *Clin. Eeg. Neurosci.* **44** (2013) 175–181.
4. M. Ahmadlou, H. Adeli and A. Adeli, Fractality analysis of frontal brain in major depressive disorder, *Int. J. Psychophysiol.* **85** (2012) 206–211.
5. U. R. Acharya, V. K. Sudarshan, H. Adeli, J. Santhosh, J. E. W. Koh and A. Adeli, Computer-Aided Diagnosis of Depression Using EEG Signals, *Eur. Neurol.* **73** (2015) 329–336.
6. U. R. Acharya, V. K. Sudarshan, H. Adeli, J. Santhosh, J. E. W. Koh, S. D. Puthankatti and A. Adeli, A novel depression diagnosis index using nonlinear features in EEG signals, *Eur. Neurol.* **74** (2015) 79–83.
7. D. Dong, Y. Wang, X. Chang, C. Luo and D. Yao, Dysfunction of large-scale brain networks in schizophrenia: A meta-analysis of resting-state functional connectivity, *Schizophr. Bull.* **44** (2017) 168–181.
8. X. Chen, G. J. Ji, C. Zhu, X. Bai, L. Wang, K. He, Y. Gao, L. Tao, F. Yu, Y. Tian and K. Wang, Neural correlates of auditory verbal Hallucinations in schizophrenia and the therapeutic response to Theta-Burst transcranial magnetic stimulation, *Schizophr. Bull.* (2018), https://doi.org/10.1093/schbul/sby054 (in press).
9. F. Yu, X. Zhou, W. Qing, D. Li, J. Li, X. Chen, G. Ji, Y. Dong, Y. Luo, C. Zhu and K. Wang, Decreased response inhibition to sad faces during explicit and implicit tasks in females with depression: Evidence from an event-related potential study, *Psychiatry Res. Neuroimag.* **259** (2017) 42–53.
10. A. M. Shepherd, K. R. Laurens, S. L. Matheson, V. J. Carr and M. J. Green, Systematic meta-review and quality assessment of the structural brain alterations in schizophrenia, *Neurosci. Biobehav. Rev.* **36** (2012) 1342–1356.
11. T. Frodl, E. Reinhold, N. Koutsouleris, M. Reiser and E. M. Meisenzahl, Interaction of childhood stress with hippocampus and prefrontal cortex volume reduction in major depression, *J. Psychiatr. Res.* **44** (2010) 799–807.
12. N. D. Woodward, H. Karbasforoushan and S. Heckers, Thalamocortical dysconnectivity in schizophrenia, *Am. J. Psychiatry* **169** (2012) 1092–1099.
13. R. C. Welsh, A. C. Chen and S. F. Taylor, Low-frequency BOLD fluctuations demonstrate altered thalamocortical connectivity in schizophrenia, *Schizophr. Bull.* **36** (2010) 713–722.
14. A. Anticevic, G. Yang, A. Savic, J. D. Murray, M. W. Cole, G. Repovs, G. D. Pearlson and D. C. Glahn, Mediodorsal and visual thalamic connectivity differ in schizophrenia and bipolar disorder with and without psychosis history, *Schizophr. Bull.* **40** (2014) 1227–1243.
15. X. Chen, M. Duan, Q. Xie, Y. Lai, L. Dong, W. Cao, D. Yao and C. Luo, Functional disconnection between the visual cortex and the sensorimotor cortex suggests a potential mechanism for self-disorder in schizophrenia, *Schizophr. Res.* **166** (2015) 151–157.
16. S. Lui, Q. Wu, L. Qiu, X. Yang, W. Kuang, R. C. Chan, X. Huang, G. J. Kemp, A. Mechelli and Q. Gong, Resting-state functional connectivity in treatment-resistant depression, *Am. J. Psychiatry* **168** (2011) 642–648.
17. W. Guo, F. Liu, J. Liu, L. Yu, J. Zhang, Z. Zhang, C. Xiao, J. Zhai and J. Zhao, Abnormal causal connectivity by structural deficits in first-episode, drug-naive schizophrenia at rest, *Schizophr. Bull.* **41** (2015) 57–65.
18. C. Luo, Y. Zhang, W. Cao, Y. Huang, F. Yang, J. Wang, S. Tu, X. Wang and D. Yao, Altered structural and functional feature of Striato-Cortical circuit in benign epilepsy with centrotemporal spikes, *Int. J. Neural Syst.* **25** (2015) 1550027.
19. H. He, C. Luo, X. Chang, Y. Shan, W. Cao, J. Gong, B. Klugah-Brown, M. A. Bobes, B. Biswal and D. Yao, The functional integration in the Sensory-Motor system predicts aging in healthy older adults, *Front Aging Neurosci* **8** (2016) 306.
20. S. Jiang, C. Luo, J. Gong, R. Peng, S. Ma, S. Tan, G. Ye, L. Dong and D. Yao, Aberrant thalamocortical connectivity in Juvenile Myoclonic epilepsy, *Int. J. Neural Syst.* **28** (2018) 1750034.
21. L. Cheng, Y. Zhu, J. Sun, L. Deng, N. He, Y. Yang, H. Ling, H. Ayaz, Y. Fu and S. Tong, Principal states of dynamic functional connectivity reveal the link between resting-state and task-state brain: An fMRI study, *Int. J. Neural Syst.* **28**(7) (2018) 1850002.
22. Y. Jiang, C. Luo, X. Li, Y. Li, H. Yang, J. Li, X. Chang, H. Li, H. Yang, J. Wang, M. Duan and D. Yao, White-matter functional networks changes in patients with schizophrenia, *Neuroimage* (2018). https://doi.org/10.1016/j.neuroimage.2018.04.018 (in press).
23. S. Ghosh-Dastidar, H. Adeli and N. Dadmehr, Voxel-based morphometry in Alzheimer's patients, *J. Alzheimers Dis.* **10** (2006) 445–447.

24. R. Goebel, A. Roebroeck, D. S. Kim and E. Formisano, Investigating directed cortical interactions in time-resolved fMRI data using vector autoregressive modeling and Granger causality mapping, *Magn. Reson. Imaging* **21** (2003) 1251–1261.
25. M. Ahmadlou and H. Adeli, Functional community analysis of brain: A new approach for EEG-based investigation of the brain pathology, *Neuroimage* **58** (2011) 401–408.
26. M. Ahmadlou and H. Adeli, Visibility graph similarity: A new measure of generalized synchronization in coupled dynamic systems, *Physica D-Nonlinear Phenomena* **241** (2012) 326–332.
27. J. Ashburner and K. J. Friston, Voxel-based morphometry–the methods, *Neuroimage* **11** (2000) 805–821.
28. R. Honea, T. J. Crow, D. Passingham and C. E. Mackay, Regional deficits in brain volume in schizophrenia: A meta-analysis of voxel-based morphometry studies, *Am. J. Psychiatry* **162** (2005) 2233–2245.
29. G. R. Ridgway, R. Omar, S. Ourselin, D. L. Hill, J. D. Warren and N. C. Fox, Issues with threshold masking in voxel-based morphometry of atrophied brains, *Neuroimage* **44** (2009) 99–111.
30. C. G. Yan, X. D. Wang, X. N. Zuo and Y. F. Zang, DPABI: Data Processing & Analysis for (Resting-State) Brain Imaging, *Neuroinformatics* **14** (2016) 339–351.
31. J. Ashburner, A fast diffeomorphic image registration algorithm, *Neuroimage* **38** (2007) 95–113.
32. J. D. Power, B. L. Schlaggar and S. E. Petersen, Recent progress and outstanding issues in motion correction in resting state fMRI, *Neuroimage* **105** (2015) 536–551.
33. J. Ashburner and K. J. Friston, Unified segmentation, *Neuroimage* **26** (2005) 839–851.
34. Z. S. Saad, S. J. Gotts, K. Murphy, G. Chen, H. J. Jo, A. Martin and R. W. Cox, Trouble at rest: How correlation patterns and group differences become distorted after global signal regression, *Brain Connect* **2** (2012) 25–32.
35. J. Geweke, Measurement of linear dependence and feedback between multiple time series, *J. Am. Stat. Assoc.* **77** (1982) 304–313.
36. A. Roebroeck, E. Formisano and R. Goebel, Mapping directed influence over the brain using Granger causality and fMRI, *Neuroimage* **25** (2005) 230–242.
37. Z. X. Zang, C. G. Yan, Z. Y. Dong, J. Huang and Y. F. Zang, Granger causality analysis implementation on MATLAB: A graphic user interface toolkit for fMRI data processing, *J. Neurosci. Methods* **203** (2012) 418–426.
38. X. Chen, Y. Jiang, L. Chen, H. He, L. Dong, C. Hou, M. Duan, M. Yang, D. Yao and C. Luo, Altered Hippocampo-Cerebello-Cortical circuit in schizophrenia by a spatiotemporal consistency and causal connectivity analysis, *Front. Neurosci.* **11** (2017) 25.
39. Y. Cai, J. Liu, L. Zhang, M. Liao, Y. Zhang, L. Wang, H. Peng, Z. He, Z. Li, W. Li, S. Lu, Y. Ding and L. Li, Grey matter volume abnormalities in patients with bipolar I depressive disorder and unipolar depressive disorder: A voxel-based morphometry study, *Neurosci. Bull.* **31** (2015) 4–12.
40. Y. Jiang, C. Luo, X. Li, M. Duan, H. He, X. Chen, H. Yang, J. Gong, X. Chang, M. Woelfer, B. B. Biswal and D. Yao, Progressive reduction in gray matter in patients with Schizophrenia assessed with MR imaging by using causal network analysis, *Radiology* **287** (2018) 633–642.
41. S. Kuhn and J. Gallinat, Resting-state brain activity in schizophrenia and major depression: A quantitative meta-analysis, *Schizophr. Bull.* **39** (2013) 358–365.
42. G. Northoff, A. Heinzel, M. de Greck, F. Bermpohl, H. Dobrowolny and J. Panksepp, Self-referential processing in our brain–a meta-analysis of imaging studies on the self, *Neuroimage* **31** (2006) 440–457.
43. L. van der Meer, S. Costafreda, A. Aleman and A. S. David, Self-reflection and the brain: A theoretical review and meta-analysis of neuroimaging studies with implications for schizophrenia, *Neurosci. Biobehav. Rev.* **34** (2010) 935–946.
44. Y. I. Sheline, D. M. Barch, J. L. Price, M. M. Rundle, S. N. Vaishnavi, A. Z. Snyder, M. A. Mintun, S. Wang, R. S. Coalson and M. E. Raichle, The default mode network and self-referential processes in depression, *Proc. Natl. Acad. Sci. USA* **106** (2009) 1942–1947.
45. J. Rabinowitz, S. Z. Levine, G. Garibaldi, D. Bugarski-Kirola, C. G. Berardo and S. Kapur, Negative symptoms have greater impact on functioning than positive symptoms in schizophrenia: Analysis of CATIE data, *Schizophr. Res.* **137** (2012) 147–150.
46. A. M. Kring, R. E. Gur, J. J. Blanchard, W. P. Horan and S. P. Reise, The Clinical Assessment Interview for Negative Symptoms (CAINS): Final development and validation, *Am. J. Psychiatry* **170** (2013) 165–172.
47. Y. Takayanagi, Y. Kawasaki, K. Nakamura, T. Takahashi, L. Orikabe, E. Toyoda, Y. Mozue, Y. Sato, M. Itokawa, H. Yamasue, K. Kasai, M. Kurachi, Y. Okazaki, M. Matsushita and M. Suzuki, Differentiation of first-episode schizophrenia patients from healthy controls using ROI-based multiple structural brain variables, *Prog. Neuropsychopharmacol. Biol. Psychiatry* **34** (2010) 10–17.
48. D. Chyzhyk, M. Grana, D. Ongur and A. K. Shinn, Discrimination of schizophrenia auditory hallucinators by machine learning of resting-state functional MRI, *Int. J. Neural Syst.* **25** (2015) 1550007.
49. V. Jumutc, P. Zayakin and A. Borisov, Ranking-based kernels in applied biomedical diagnostics using

a support vector machine, *Int. J. Neural Syst.* **21** (2011) 459–473.
50. M. Grana, L. Ozaeta and D. Chyzhyk, Resting State Effective Connectivity Allows Auditory Hallucination Discrimination, *Int. J. Neural Syst.* (2017) 1750019.
51. H. He, M. Yang, M. Duan, X. Chen, Y. Lai, Y. Xia, J. Shao, B. B. Biswal, C. Luo and D. Yao, Music intervention leads to increased insular connectivity and improved clinical symptoms in schizophrenia, *Front. Neurosci.* **11** (2017) 744.
52. M. J. Muller, A. Szegedi, H. Wetzel and O. Benkert, Depressive factors and their relationships with other symptom domains in schizophrenia, schizoaffective disorder, and psychotic depression, *Schizophr. Bull.* **27** (2001) 19–28.
53. C. Kohler, C. L. Swanson, R. C. Gur, L. H. Mozley and R. E. Gur, Depression in schizophrenia: II. MRI and PET findings, *Biol. Psychiatry* **43** (1998) 173–880.
54. K. H. Karlsgodt, D. Sun, A. M. Jimenez, E. S. Lutkenhoff, R. Willhite, T. G. van Erp and T. D. Cannon, Developmental disruptions in neural connectivity in the pathophysiology of schizophrenia, *Dev Psychopathol* **20** (2008) 1297–1327.
55. D. A. Fair, D. Bathula, K. L. Mills, T. G. Dias, M. S. Blythe, D. Zhang, A. Z. Snyder, M. E. Raichle, A. A. Stevens, J. Nigg T. and B. J. Nagel, Maturing thalamocortical functional connectivity across development, *Front. Syst. Neurosci.* **4** (2010) 10.
56. L. Schilbach, F. Hoffstaedter, V. Muller, E. C. Cieslik, R. Goya-Maldonado, S. Trost, C. Sorg, V. Riedl, R. Jardri, I. Sommer, L. Kogler, B. Derntl, O. Gruber and S. B. Eickhoff, Transdiagnostic commonalities and differences in resting state functional connectivity of the default mode network in schizophrenia and major depression, *Neuroimage Clin.* **10** (2016) 326–335.
57. Y. Yu, H. Shen, L. L. Zeng, Q. Ma and D. Hu, Convergent and divergent functional connectivity patterns in schizophrenia and depression, *PLoS One* **8** (2013) e68250.
58. A. Anticevic, M. W. Cole, G. Repovs, J. D. Murray, M. S. Brumbaugh, A. M. Winkler, A. Savic, J. H. Krystal, G. D. Pearlson and D. C. Glahn, Characterizing thalamo-cortical disturbances in schizophrenia and bipolar illness, *Cereb. Cortex* **24** (2014) 3116–3130.
59. G. Wagner, K. Koch, C. Schachtzabel, C. C. Schultz, C. Gaser, J. R. Reichenbach, H. Sauer, K. J. Bar and R. G. Schlosser, Structural basis of the fronto-thalamic dysconnectivity in schizophrenia: A combined DCM-VBM study, *Neuroimage Clin.* **3** (2013) 95–105.
60. S. Marenco, J. L. Stein, A. A. Savostyanova, F. Sambataro, H. Y. Tan, A. L. Goldman, B. A. Verchinski, A. S. Barnett, D. Dickinson, J. A. Apud, J. H. Callicott, A. Meyer-Lindenberg and D. R. Weinberger, Investigation of anatomical thalamo-cortical connectivity and FMRI activation in schizophrenia, *Neuropsychopharmacology* **37** (2012) 499–507.
61. D. Arnone, D. Job, S. Selvaraj, O. Abe, F. Amico, Y. Cheng, S. J. Colloby, J. T. O'Brien, T. Frodl, I. H. Gotlib, B. J. Ham, M. J. Kim, P. C. Koolschijn, C. A. Perico, G. Salvadore, A. J. Thomas, M. J. Van Tol, N. J. van der Wee, D. J. Veltman, G. Wagner and A. M. McIntosh, Computational meta-analysis of statistical parametric maps in major depression, *Hum. Brain Mapp.* **37** (2016) 1393–1404.
62. P. Fusar-Poli, A. Placentino, F. Carletti, P. Landi, P. Allen, S. Surguladze, F. Benedetti, M. Abbamonte, R. Gasparotti, F. Barale, J. Perez, P. McGuire and P. Politi, Functional atlas of emotional faces processing: A voxel-based meta-analysis of 105 functional magnetic resonance imaging studies, *J. Psychiatry Neurosci.* **34** (2009) 418–432.
63. C. J. Stoodley and J. D. Schmahmann, Evidence for topographic organization in the cerebellum of motor control versus cognitive and affective processing, *Cortex* **46** (2010) 831–844.
64. S. M. Smith, K. L. Miller, G. Salimi-Khorshidi, M. Webster, C. F. Beckmann, T. E. Nichols, J. D. Ramsey and M. W. Woolrich, Network modelling methods for FMRI, *Neuroimage* **54** (2011) 875–891.
65. S. A. Akar, S. Kara, F. Latifoglu and V. Bilgic, Analysis of the complexity measures in the EEG of schizophrenia patients, *Int. J. Neural Syst.* **26** (2016) 1650008.
66. F. Li, F. Wang, L. Zhang, T. Zhang, R. Zhang, L. Song, H. Li, Y. Jiang, Y. Tian and Y. Zhang, The dynamic brain networks of motor imagery: Time-varying causality analysis of scalp EEG, *Int. J. Neural Syst.* (2018). https://doi.org/10.1142/S0129065718500168 (in press).
67. G. F. Busatto, Structural and Functional Neuroimaging Studies in Major Depressive Disorder With Psychotic Features: A Critical Review, *Schizophr. Bull.* **39** (2013) 776–786.